Global Biogeochemical Cycles

RESEARCH ARTICLE
10.1029/2020GB006647

Special Section:
Fire in the Earth System

The Relevance of Pyrogenic Carbon for Carbon Budgets From Fires: Insights From the FIREX Experiment

Cristina Santin[1,2], Stefan H. Doerr[3], Matthew W. Jones[3,4], Agustin Merino[5], Carsten Warneke[6,7], and James M. Roberts[6]

[1]Biosciences Department, Swansea University, Swansea, UK, [2]Research Unit of Biodiversity (CSIC, UO, PA), University of Oviedo, Mieres, Spain, [3]Geography Department, Swansea University, Swansea, UK, [4]Tyndall Centre for Climate Change Research, University of East Anglia, Norwich, UK, [5]Soil Science and Agricultural Chemistry Department, University of Santiago de Compostela, Lugo, Spain, [6]Chemical Sciences Division, NOAA Earth System Research Laboratory (ESRL), Boulder, CO, USA, [7]Cooperative Institute for Research in Environmental Sciences, University of Colorado Boulder, Boulder, CO, USA

Key Points:
- Most carbon emission calculations are based on the "consumed biomass" approach instead of the "burnt carbon" approach
- Based on laboratory burns, we demonstrate the "consumed biomass" approach overestimates carbon emissions by 2–27%
- The burnt carbon not emitted remains in situ as pyrogenic carbon, which can act as a carbon sink due to enhanced environmental recalcitrance

Supporting Information:
- Supporting Information S1

Correspondence to:
C. Santin,
c.santin@swansea.ac.uk

Citation:
Santin, C., Doerr, S. H., Jones, M. W., Merino, A., Warneke, C., & Roberts, J. M. (2020). The relevance of pyrogenic carbon for carbon budgets from fires: Insights from the FIREX experiment. *Global Biogeochemical Cycles*, *34*, e2020GB006647. https://doi.org/10.1029/2020GB006647

Received 24 APR 2020
Accepted 18 AUG 2020
Accepted article online 21 AUG 2020

Abstract Vegetation fires play an important role in global and regional carbon cycles. Due to climate warming and land use shifts, fire patterns are changing and fire impacts increasing in many of the world's regions. Reducing uncertainties in carbon budgeting calculations from fires is therefore fundamental to advance our current understanding and forecasting capabilities. Here we study 20 chamber burns from the FIREX FireLab experiment, which burnt a representative set of North American wildland fuels, to assess the following: (i) differences in carbon emission estimations between the commonly used "consumed biomass" approach and the "burnt carbon" approach; (ii) pyrogenic carbon (PyC) production rates; and (iii) thermal and chemical recalcitrance of the PyC produced, as proxies of its biogeochemical stability. We find that the "consumed biomass" approach leads to overestimation of carbon emissions by 2–27% (most values between 2% and 10%). This accounting error arises largely from not considering PyC production and, even if relatively small, can therefore have important implications for medium- and long-term carbon budgeting. A large fraction (34–100%) of this PyC was contained in the charred fine residue, a postfire material frequently overlooked in fire carbon research. However, the most recalcitrant PyC was in the form of woody charcoal, with estimated half-lives for most samples exceeding 1,000 years. Combustion efficiency was relatively high in these laboratory burns compared to actual wildland fire conditions, likely leading to lower PyC production rates. We therefore argue that the PyC production values obtained here, and associated overestimation of carbon emissions, should be taken as low-end estimates for wildland fire conditions.

Plain Language Summary Wildfires release substantial amounts of carbon into the atmosphere with direct implications for climate change and air quality. However, not all the carbon from the burnt vegetation is emitted; a fraction of it remains on the ground as charcoal (pyrogenic carbon—PyC). PyC is more resistant to degradation than unburnt vegetation, and the carbon it contains can be stored in soils and sediments for long periods of time instead of going back to the atmosphere. Most current carbon emissions estimations do not take PyC production into account and assume that all carbon burnt is emitted into the atmosphere. Here we quantify carbon emissions and PyC production during the FIREX laboratory burns (Missoula Fire Lab, October 2016), where a range of North American vegetation types (e.g., chaparral shrubs, conifer trees) were burnt to study their emissions. We found that the current way of calculating carbon emissions can lead to an overestimation of carbon emissions of between 2% and 27%. We also found that the PyC produced during burning is mostly held not in big woody pieces of charcoal but instead in small charred particles, which are often not accounted for in wildfire research.

1. Introduction

Vegetation fires burn about 3–5 $\times$ 10^6 km^2 every year around the world (Van Der Werf et al., 2017). They exert substantial impacts on regional to global biogeochemical cycles across a broad range of ecosystems and temporal scales. One of their most important impacts is on the carbon (C) cycle. Vegetation fires currently emit an estimated 2.2 $\times$ 10^{15} Pg of C directly into the atmosphere per year (Van Der Werf et al., 2017). In addition, they redistribute C between ecosystem pools by, for example, transferring C from the

aboveground living to the dead vegetation pools (Yang et al., 2018). From an ecological perspective, fire can change ecosystem succession or even result in shifts between ecosystem types, consequently altering ecosystem C storage capacity (Gao et al., 2018; Millar & Stephenson, 2015). Fire can also lead to changes in the soil C stocks, either by direct combustion of soil organic matter or, more commonly, via indirect effects through enhancement of soil erosion or land-cover changes (Santin & Doerr, 2019; Santín & Doerr, 2016).

From an immediate temporal perspective, the most substantial impact of fire on the C cycle is through emissions. During burning, part of the C stored in the vegetation is rapidly released into the atmosphere, both as gases (e.g., CO_2, CO, and CH_4, and other volatile organic compounds, VOCs) and aerosols (e.g., black carbon, brown carbon) (Akagi et al., 2011; Bond et al., 2013). These pyrogenic atmospheric species play important roles in the atmosphere's chemistry influencing air quality and Earth's radiative balance (Bond et al., 2013; Ditas et al., 2018; Ramanathan & Carmichael, 2008). As global warming and anthropogenic land use change continue to affect environmental conditions at the land surface, including temperature, humidity, drought frequency, and ignition risk, it is projected that the significance of fire in driving biogeochemical cycles will increase in many regions across the world (Abatzoglou et al., 2018; Turco et al., 2018). Consequently, there is a growing appreciation that precise measurements of fire effects on terrestrial C stocks are critical to projecting the future global dynamics of C in the Earth System (Landry & Matthews, 2017; Surawski et al., 2016; Yang et al., 2015). Most exercises for calculating, modeling, and forecasting fire emissions use the "consumed biomass" approach, which assumes that all burnt C is emitted as gases and aerosols (Surawski et al., 2016). The C released into the atmosphere is, therefore, calculated by multiplying the C concentration in the fuel biomass by the amount of fuel burnt (i.e., consumed by fire). However, this approach is biased, as it does not account for the portion of the C burnt by the fire not emitted into the atmosphere but remaining as burnt residues on the ground or on standing vegetation (i.e., charred fine residues, charcoal, and charred vegetation; Surawski et al., 2016). Most of this burnt C remaining on site is present in organic forms, although some may be present as inorganic C (mostly carbonates) (Bodí et al., 2014). Fire-derived organic C is usually known as pyrogenic C. The term pyrogenic carbon (PyC) encompasses the whole range of organic materials chemically produced/transformed by charring, from lightly charred vegetation to charcoal and soot (Bird et al., 2015). Compared to their unburnt precursors, PyC materials are commonly enriched in C, more chemically and thermally recalcitrant, and with resulting longer mean residence times in the environment (Santín et al., 2016). PyC production from fires is therefore regarded as a globally significant C sink mechanism (Jones et al., 2019; Landry & Matthews, 2017; Santín et al., 2015). It is important to note though that PyC products from vegetation fires are both chemically and physically variable, therefore spanning a wide range of C sequestration potentials (Bird et al., 2015; McBeath et al., 2013; Santín et al., 2017; Schneider et al., 2013).

Despite its potential relevance, the PyC component is not yet routinely accounted for in fire-enabled global vegetation models that are used in Earth System Models (ESMs) for regional and global C budget assessments and climate projections (Hantson et al., 2016; Jones et al., 2019). The inclusion of PyC in ESMs is indeed rare (Landry & Matthews, 2017) and lags far behind the inclusion of pyrogenic aerosol emissions (e.g., black carbon) for which functionality has been developed in all leading global-scale models (e.g., Bond et al., 2013; Koch et al., 2009). One reason for this seems to be a lack of connection between research addressing the atmospheric and the terrestrial components of C fluxes from fires (Ottmar, 2014; Santín et al., 2016). As one of the first steps in bridging this gap, we report here on the estimates of PyC production, and chemical properties related to its C sequestration potential, during the laboratory phase of the NOAA Fire Influence on Regional and Global Environments Experiment (FIREX Firelab).

While atmospheric scientists involved in the NOAA FIREX project targeted improved particle- and gas-phase emission factors for use in atmospheric models (as reported by Koss et al., 2018; Li et al., 2019; Sekimoto et al., 2018; Selimovic et al., 2018, among others), we conducted a parallel analysis of the residual materials remaining after a series of 20 experimental laboratory burns. We quantified the PyC and inorganic C contents, as well as H and O concentrations and the thermal recalcitrance of the different forms of C (assessed by thermogravimetry-differential scanning calorimetry). These data, in combination with corresponding analyses of the fuel components, allow us to provide full estimations of the C budgets, including PyC production, for these laboratory fires and to quantify bias arising from applying the commonly used "consumed biomass" approach when calculating C emissions.

Figure 1. Example of a FIREX 2016 FireLab chamber burn with a ~1 × 1 m fuel bed, here comprising mixed longleaf pine fuel (Fires 96 and 97 in Table 1). The postfire components (right) included unburnt fuels, charcoal, and charred fine residues (i.e., <1 cm size).

2. Materials and Methods

2.1. The FIREX 2016 FireLab Experiment

During the FIREX laboratory experiment (Octobe-November 2016; USDA Fire Sciences Laboratory, Missoula, US), a range of fuel types representative of the most fire-prone ecosystems in the USA (e.g., conifer forests, chaparral, sagebrush) were burnt and their emissions extensively monitored. A total of 107 fuel beds (~1 × 1 m) were burned, with the first 75 fires being carried out as "stack burns" (online emission monitoring) and the final 32 as "chamber burns" (emissions monitored once the burn was complete and the room full of smoke) (Figure 1). For more detailed information on the general experimental settings and procedures, see Selimovic et al. (2018).

For the present study, 20 of the 32 chamber burns were utilized (Table 1). These 20 laboratory burns were chosen as they covered the range of U.S. fuels used in the wider FIREX 2016 FireLab experiment, including fuels typical of Californian chaparral and of several types of conifer forests from both western and eastern U. S. states (Table 1). Most of the studied fuel beds simulated, at small scales, the fuel structure and composition burnt in real field-scale vegetation fires. For the shrubby vegetation types (i.e., ceanothus, sagebrush, chamise, and manzanita, Table 1), the aerial parts of the shrubs were burnt (avoiding very thick branches and/or stems). For the forest vegetation types (i.e., lodgepole, ponderosa, and longleaf pines and Douglas-fir), "mixed fuel beds" were used. These replicated real forest stands and, therefore, included all fuel components that contribute most to the combustion process during wildfire: duff, litter, dead/down wood (DW), understory, herbs, and canopy in realistic mass proportions (Figure 1 and Table 1). As these were small-scale burns, stems of standing timber and big DW pieces (>7.6 cm diameter) were not included. To provide a better understanding of specific fuel components, litter, and duff layers, as well as the canopy, some relevant conifer species were also burnt separately (Table 1). In addition, a bed of excelsior (wood wool) was included as a simplified fuel type (Table 1). For a detailed description of the fuel components and their masses in each fire, see Figure S1 in Selimovic et al. (2018).

Before each burn, the different prefire fuel components were weighed independently and samples from each of them taken for further analysis. When present, canopy and shrub fuel components were classified (and weighed separately) as part of two diameter classes: <0.5 cm diameter, which comprised leaves/needles and thin twigs, and >0.5 cm diameter, which were thicker branches. The DW fuel component was also

Table 1
Description of the Fuel Bed Types Used in This Study

Fuel bed type		Fuel description	Fire number
1	Excelsior	Wood wool	82
2	Ceanothus	*Ceanothus* sp. shrubs (aerial parts, including leaves and branches)	89
3	Sagebrush	*Artemisia* sp. shrubs (aerial parts, including leaves and branches)	85
4	Chamise	*Adenostoma fasciculatum* shrubs (aerial parts, including leaves and branches)	77, 84, 94
5	Manzanita	*Arctostaphylos* sp. shrubs (aerial parts, including leaves and branches)	76, 91
6	Juniper canopy	Aerial parts of *Juniperus* sp. (branches and leaves)	88
7	Lodgepole pine canopy	Aerial parts of *Pinus contorta* (branches and leaves)	87
8	Lodgepole pine mixed fuel	*Pinus contorta* stand, with duff, litter, down wood, shrub, herbs and canopy	79, 86
9	Douglas-fir mixed fuel	*Pseudotsuga menziesii* stand, with duff, litter, down wood, shrub, and canopy	80
10	Ponderosa pine mixed fuel	*Pinus ponderosa* stand, with duff, litter, down wood, shrub, and canopy	78
11	Longleaf pine mixed fuel	*Pinus palustris* stand, with duff, litter, down wood, shrub, herbs, and canopy	96, 97
12	Ponderosa pine litter	Litter of *Pinus ponderosa*	95
13	Subalpine fir duff	Duff of *Abies lasiocarpa*	90
14	Engelmann spruce duff	Duff of *Picea engelmannii*	83, 92

Note. Some of the fuel types were used in more than one fire ("Fire number" column). The fire number is the one originally assigned in the FIREX 2016 Firelab experiment (more details in Selimovic et al., 2018).

split into "small DW" (<2.5 cm diameter, i.e., <100 hr fuels) and "coarse DW" (2.5–7.6 cm diameter, i.e., 100 hr fuels). Six K-type thermocouples (Lascar, Easylog, USA) were placed at 3–5 cm height ~25 cm apart along two lines in the fuel bed perpendicular to the ignition line to record temperatures during the burns. From these thermocouples, the maximum temperature (°C) recorded and the residence time (in seconds) above 300°C were extracted as descriptors of fuel charring and PyC formation (Doerr et al., 2018; Santín et al., 2017). After the burns and once the residues left had sufficiently cooled, the materials remaining on the fuel bed were collected and classified into different types (i.e., unburnt fuels, charred fuels/charcoal, and charred fine residues) (Figure 1). When possible, postfire components were also separated according to the type of fuel components that were present before the fire. For example, if both DW and woody canopy were present, the charcoal derived from both components was differentiated and sampled separately as "charcoal from canopy" and "charcoal from DW." Postfire components were then weighed and representative subsamples of each of them taken. All samples (from prefire and postfire components) were oven-dried at 100°C until constant weight to determine their dry mass and moisture contents (Norum & Miller, 1984). The dried subsamples were ground for further analyses.

It is important to note that what we define here as "charred fine residues" is equivalent to the term "wildland fire ash" widely used in postfire hydrology and soil research ("the fine (<1 cm) particulate residue left on the ground after the fire"; Bodí et al., 2014, p. 104). It consists not only of mineral inorganic, but also of charred organic materials, and can therefore be an important postfire stock of PyC (Santín et al., 2012). Meanwhile, the term "charcoal" is given here to all charred woody pieces >1 cm in diameter and whose entire cross sections were visibly charred (blackened). When a woody piece in the >1 cm class was not completely charred (e.g., an unburnt woody core surrounded by a charred exterior), the charred fraction was scraped from the unburnt wood using a blade and its mass determined and included in the "charcoal" component. Charcoal pieces <1 cm (completely charred through) were included within the "charred fine residue" component. Woody pieces <1 cm but only charred on the outside were very infrequent but, when present, they were considered as unburnt fuel.

2.2. Elemental Analyses

Total C and hydrogen (H) contents (%) for a representative subset of fuel, charcoal, and "charred fine residue" samples (total $n = 78$) were determined using a LECO elemental analyzer. For "charred fine residue" samples, the organic C content was also determined using the LECO after treating them with hydrochloric acid to remove carbonates. Inorganic C content was then calculated as the difference between total and organic C (after accounting for mass loss during the hydrochloric acid treatment). For the rest of the components analyzed (i.e., unburnt fuels and charcoals), inorganic C content was considered as negligible and, therefore, total C taken as equivalent to organic C. For the charcoal samples, oxygen (O) content (%) was

measured with a FISONS elemental analyzer (Model EA 1108, Fisons Instruments, Beverly, MA, USA). Every one in five samples were analyzed in duplicate with variability between these two replicates being always <3% for C and <5% for H and O values.

For the charcoal samples, H:C and O:C molar ratios were calculated to allow plotting them on a van Krevelen diagram (see section 3.4), and O:C ratios were used to estimate half-life ($t_{1/2}$) ranges according to the classification of Spokas (2010): O:C < 0.2 = $t_{1/2}$ > 1,000 yr; O:C 0.2–0.6 = 100 yr < $t_{1/2}$ < 1,000 yr; O:C > 0.6 = $t_{1/2}$ < 100 yr.

2.3. Thermogravimetry-Differential Scanning Calorimetry

Thermogravimetry-differential scanning calorimetry (TG-DSC) was carried out for a selected subset of samples (n = 32) using a Mettler Toledo instrument, calibrated using indium samples (mp: 156.6°C). Samples were analyzed in duplicate, four milligrams of sample were placed in aluminum pans under dry air (under O_2 flux; flow rate, 50 m L^{-1}) and heated from 50 to 600°C at a heating rate of 10°C min^{-1}. For each DSC thermograph, the area in the 150–600°C region, where combustion of organic matter occurs, was divided into three temperature sections representing different levels of resistance to thermal oxidation (Merino et al., 2015): thermally labile organic matter, mainly comprising carbohydrates, proteins, and other labile aliphatic compounds (150 < T_1 < 375°C); thermally recalcitrant organic matter, such as lignin or other polyphenols (375 < T_2 < 475°C); and highly thermally recalcitrant organic matter, such as polycondensed aromatic forms (475 < T_3 < 600°C). The resulting partial heats of combustion representing these three regions were calculated as Q1, Q2, and Q3, respectively. Here, Q3 (%) is used as an indicator of thermally recalcitrant organic matter which has also proven to be more resistant to microbial degradation than material falling into regions Q1 and Q2 (Campo & Merino, 2016). In addition, the recalcitrance index R_{50} (Harvey et al., 2012) was calculated from the TG thermographs as: $R_{50,x} = T_{50,x}/T_{50,\text{graphite}}$; where $T_{50,x}$ is the temperature value at which 50% of the total mass of the x sample is lost, and $T_{50,\text{graphite}}$ the temperature value at which 50% of the total mass of graphite is lost. For graphite, Alfa Aesar graphite powder (99.9% purity) was used with a TG-DSC cutoff temperature of 1,100°C. $T_{50,\text{graphite}}$ was 823°C. The studied materials were classified into the following recalcitrance/C sequestration potential classes according to Harvey et al. (2012): Class A: R_{50} < 0.50; Class B: 0.50 ≤ R_{50} < 0.70; Class C: R_{50} > 0.70.

2.4. Carbon Budget Calculations

Here we use the term "pyrogenic carbon" (PyC) to account for all the fuel organic C that has been blackened, and thus chemically altered by fire (Bird & Ascough, 2012). This visual identification of PyC is broad, encompassing the whole range of PyC materials remaining in situ after a fire (Santín et al., 2015). We therefore consider all the C in charcoal/charred (i.e., blackened) fuels, as well as all the organic C in the "charred fine residue" component, as PyC. It is important to note that we only quantify the PyC remaining on the ground, missing the airbone PyC particles transported off-site in the smoke column (e.g., char- and soot-black carbon; Han et al. 2010). This airborne PyC component is therefore considered here as part of the C emitted. It is generally a minor mass fraction compared to the PyC remaining on the ground (Santín et al., 2016).

For each of the 20 burns, mass, and C loads (g m^{-2}) in the different prefire fuel components and postfire uncharred fuel, charred fine residue and charcoal components were calculated using the dry mass and measured C concentrations for each of the prefire and postfire components. C emitted values (g m^{-2}) were then estimated as the difference between prefire fuel C amount and the amount of C in the remaining postfire components (i.e., C emitted = C in prefire fuels − C in postfire uncharred fuel − C in charcoal − C in charred fine residue; all in g m^{-2}). (Note that C in postfire uncharred fuels were considered to be the same as in prefire fuels and, therefore, not measured.)

The conversion rate (%) of C in fire-affected or "burnt" fuel (carbon burnt: CB) to pyrogenic carbon was estimated according to Santín et al. (2015) as 100 × (PyC/CB), with CB being the sum of PyC + inorganic C in charred fine residue + C emitted. Note that in Santín et al. (2015) the term "C affected—CA" was used instead of "C burnt—CB". Both terms are interchangeable (i.e., CB = CA) and in the present study we use "C burnt" consistently to follow the terminology in Surawski et al. (2016). The proportion (%) of PyC to C emitted was also calculated as 100 × (PyC/C emitted). The combustion completeness is "the fraction of the total biomass that was exposed to a fire that actually burned" (Akagi et al., 2011) and, therefore, the combustion completeness in terms of C was calculated as the difference (in %) of the fuel C before and

Table 2
Description of Burning Conditions for the Fuel Bed Types Assessed in This Study

Fuel bed type		Fire number	Fire type	Max. T (°C)	Time >300°C (s)	Fire description
1	Excelsior	82	Flaming	781	149 ± 76	Very complete combustion; mostly fine residue left
2	Ceanothus	89	Flaming	876	128 ± 164	High combustion efficiency; some unburnt branches; mostly fine residue
3	Sagebrush	85	Flaming	1,012	199 ± 305	High combustion efficiency; some unburnt branches; mostly fine residue
4	Chamise	77, 84, 94	Flaming	1,017	154 ± 67	Very complete combustion; mostly fine residue left
5	Manzanita	76, 91	Flaming	1,053	181 ± 109	Very complete combustion; mostly fine residue left
6	Juniper canopy	88	Flaming	939	59 ± 36	Very complete combustion; mostly fine residue left
7	Lodgepole pine canopy	87	Flaming	699	51 ± 16	High combustion efficiency; some unburnt branches left
8	Lodgepole pine mixed fuel	79, 86	Flaming	857	170 ± 15	Some unburnt material left, charcoal and fine residue left
9	Douglas-fir mixed fuel	80	Flaming	802	133 ± 100	Some unburnt material left, charcoal and fine residue left
10	Ponderosa pine mixed fuel	78	Flaming	740	47 ± 29	Some unburnt material left, charcoal and fine residue left
11	Longleaf pine mixed fuel	96, 97	Flaming	834	188 ± 151	High amounts of charcoal and black fine residue left
12	Ponderosa pine litter	95	Flaming	946	164 ± 140	Very complete combustion; mostly fine residue left
13	Subalpine fir duff	90	Smoldering	603	1,412 ± 345	Smoldering fire, very complete combustion; mostly fine residue left
14	Engelmann spruce duff	83, 92	Smoldering	502	No data	Smoldering fire, very complete combustion; mostly fine residue left

Note. Some of the fuel types were used in several fires (Fire number). The Max. T corresponds to the hottest temperature registered during that fire(s). Time >300°C is the average residence time (in seconds) above 300°C for that fire(s) (six thermocouples used in each fire, see section 2.1).

after fire. We would like to note here that this is the same as calculating C combustion completeness as the percentage of CB (i.e., inorganic C + PyC + C emitted) divided by the prefire C mass.

The approach used above to calculate the C emitted is equivalent to the "burnt carbon" approach reported in Surawski et al. (2016). This approach enables the C burnt by the fire to be correctly partitioned into atmospheric emissions and PyC (and inorganic C) remaining on the ground. In addition, the C emitted using the "consumed biomass" approach reported in Surawski et al. (2016) was also calculated (C emitted = C in prefire fuels − C in postfire uncharred fuel; all in g m^{-2}). The percent overestimation of C emissions when using the "consumed biomass" approach instead of the "burnt carbon" approach was calculated as $(Cemitted_{ConsumedBiomass}\text{-}Cemitted_{BurntCarbon})/Cemitted_{BurntCarbon} \times 100$.

Relationships between C stocks in prefire and postfire components were investigated through correlation analysis. The function *cor* of R statistics (R Core Team, 2019) was used to compute correlations based on pairwise complete observations, whereas the Corrplot package (Wei & Simko, 2017) was used to plot these correlations graphically. Correlations were calculated both for absolute C stocks and for the various ratios of these C stocks (Figure S1 in the supporting information).

3. Results

3.1. Burning Conditions During the FIREX 2016 FireLab Experiment

Most of the 20 burns monitored resulted in intensely flaming fires (Table 2, Figure 1). The burning of shrub, canopy, and litter fuels resulted in maximum fuel bed temperatures ranging from 699–1,053°C and average residence times >300°C of less than 200 s (Fuels 1–7 and 12, Table 2). These fuels burned with high combustion completeness and the majority of the burnt residues left on the ground were fine and light-colored (Tables 2 and 3). Lower maximum temperatures (740–857°C) were recorded in the mixed fuel beds, resulting in greater production of charcoal and dark charred fine residues (Fuels 8–11, Table 2). Burning of these mixed fuel beds was also relatively short (residence times >300°C of less than 200 s; Table 2). The duff fuel beds burnt mostly under smoldering (nonflaming) conditions, with relatively low maximum temperatures (502–603°C), but very long residence times (>300°C of around 1,400 s; Table 2), what also resulted in very complete consumption of the fuels, leaving behind mostly fine gray residues (Fuels 12–14, Tables 2 and 3).

Table 3
Fire and Carbon Parameters for the 14 Fuel Bed Types Studied (See Section 2.4 for Calculations)

Fuel bed type		Fire number	InorganicC/ CBurnt (%)	PyC/ CBurnt (%)	PyC/ CEmitted (%)	PyC/ prefire C (%)	CEmitted/ prefire C (%)	C combustion completeness (%)	Overestimation C emissions with consumed biomass approach (%)
1	Excelsior	82	0.2	1.5	1.6	1.5	98.3	100.0	1.8
2	Ceanothus	89	0.6	1.6	1.6	1.2	73.2	74.8	2.2
3	Sagebrush	85	0.3	2.0	2.1	1.6	76.8	78.6	2.4
4	Chamise	77, 84, 94	0.5	3.4	3.6	3.2	91.3	95.0	4.1
5	Manzanita	76, 91	0.5	1.1	1.1	1.0	95.3	96.8	1.6
6	Juniper canopy	88	0.7	2.1	2.2	1.5	69.5	71.5	2.9
7	Lodgepole pine canopy	87	0.3	1.2	1.3	0.7	57.4	58.3	1.5
8	Lodgepole pine mixed fuel bed	79, 86	0.2	10.2	11.4	7.5	66.0	73.7	11.6
9	Douglas-fir mixed fuel bed	80	0.4	7.2	7.8	4.9	62.4	67.5	8.2
10	Ponderosa pine mixed fuel bed	78	0.0	9.3	10.2	7.0	69.0	76.1	10.2
11	Longleaf pine mixed fuel bed	96, 97	0.3	21.0	26.7	18.1	67.8	86.2	27.0
12	Ponderosa pine litter	95	1.8	6.7	7.3	6.6	90.9	99.2	9.2
13	Subalpine fir duff	90	0.0	4.2	4.4	4.0	92.2	96.3	4.4
14	Engelmann spruce duff	83, 92	0.4	3.9	4.2	3.9	94.9	99.1	4.5

Note. For fuel bed types that were used in more than one fire, the average values are displayed. For other parameters and raw data see supporting information Table S3.

3.2. Inorganic Carbon Production in the FIREX 2016 FireLab Experiment

In all fires, the proportion of inorganic C produced in terms of CB was very low (<2%), with inorganic C production being always lower than PyC production (Table 3). Fuels that burnt more completely, such as those of chaparral, tended to produce more inorganic C and less PyC (Table 3). This is in agreement with previous studies that link more complete combustion with greater organic C release (as gases or aerosols) and a greater fraction of the residual C in carbonates (Bodí et al., 2014). However, no significant correlation was found between inorganic C and PyC production in our data set (Figure S1).

3.3. Pyrogenic Carbon Production in the FIREX 2016 FireLab Experiment

Total PyC production was very variable among the experimental fires, ranging from 1.1% to 21.0% of the CB (Table 3). The fuel beds composed of predominantly woody fine fuels (shrub and canopy, fuel types, #1–7) burnt with a very complete combustion under flaming conditions and produced, overall, the lowest proportion of PyC (1.1–3.4% PyC/CB). The duff fuel beds (#13 and 14), which were also fine fuels but burnt mostly under smoldering conditions (Table 2), produced slightly more PyC than the other fine fuel beds, although the values were still low (3.9–4.2% PyC/CB). The only litter fuel studied independently (#12) produced more PyC than the other fine fuels (6.7% PyC/CB, Table 3). The mixed fuel beds (#8–11) showed the highest PyC production (6.3–21.0%) and generated substantial amounts of woody charcoal and dark charred fine residues (Table 2). It is notable that the fraction of CB converted to PyC during the two longleaf pine mixed fuel fires was more than double that of any other fire (Table 3).

Figure 2 shows both the proportion of C in the different prefire fuel bed components (Figure 2a) and the proportion of PyC (%PyC/CB) in the postfire components for the 14 fuel bed types studied (Figure 2b). The majority of PyC (54–100%) was found in the "charred fine residue" component, in all cases except the ceanothus (41%) and the juniper canopy burns (34%) (#2 and 6 in Figure 2b). Canopy and shrubs fuel beds, even those with an important woody component (Figure 2a), were generally highly consumed, and therefore most of the PyC derived from them became part of the charred fine residues (except in Fuels #2 and 6), rather than remaining as recognizable pieces of charred canopy or charcoal (Figure 2b). Fine fuels such as excelsior,

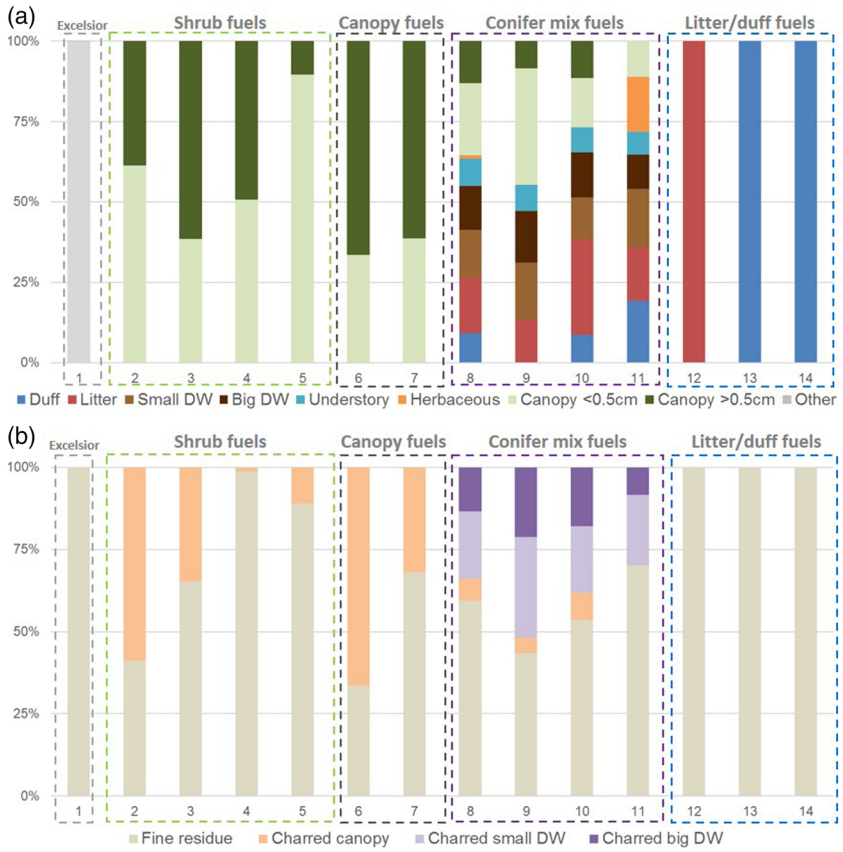

Figure 2. Relative quantities of (a) prefire carbon (%) in each fuel component of the 14 fuel bed types, and (b) pyrogenic carbon (%) in each postfire component. Numbers on the *x* axes refer to the 14 types of fuel beds studied (see Tables 2 and S3). Note that "charred canopy" is charcoal derived from small twigs and branches (so no leaf/needle material). "Charred big DW" is charcoal produced in 100 hr woody fuels (i.e., 2.5–7.6 cm diameter) and "charred small DW" is charcoal derived from <100 hr woody fuels (<2.5 cm diameter).

litter, and duff only produced fine residues and thus contributed only to the postfire "charred fine residue" component (Figure 2b). The mixed fuel beds were associated with the most diverse distribution of C components both before and after the fire (Fuels #8–11, Figures 2a and 2b). In these mixed fuel beds, the canopy components were also highly consumed, as in the case of the fuel beds with single fuel types, and, therefore, most of the PyC attributable to these sources was found in the "charred fine residue" component. The DW fuel components produced a substantial quantity of woody charcoal, with PyC in these products contributing notably to total PyC formed (Figure 2b). It is, however, important to consider that DW may have also produced finer PyC that would have contributed to the PyC stock in the "charred fine residue" component.

No significant correlations were observed between PyC production (%PyC/CB) and any of the other parameters analyzed, such as %CB, %Cemitted, %IC, combustion completeness, or maximum temperature recorded (Figure S1).

3.4. Chemical Characteristics of Carbon Components in the FIREX 2016 FireLab Experiment

The fuel components used in these fires contained 48–51% organic C with a low variability between the different types of fuel (Table 4). The only exception was duff, which, in the present study, always contained a substantial proportion of mineral soil and, thus, held lower concentrations of organic C (32 ± 12%).

The organic C content in the "charred fine residue" component was always lower than that in the fuel components from which it originated (7–39%), with a large variability both between and within charred fine residue types (Table 4). The charred fine residue types with the highest concentrations of organic C were those

Table 4
Average Concentrations (%) of Organic Carbon (OC), Inorganic Carbon (IC), Hydrogen (H) and Oxygen (O) in Different Types of Samples (Fuels, Charred Fine Residues and Charcoals) for the Range of Fuel Bed Types Studied

Sample type	Description	Fuel bed types	N. of samples	%OC	%IC	%H	%O
Fuel	Canopy <0.5 cm	2,3,4,5,6,7-8,9,11	9	49.4	n.a.	6.5	n.a.
				1.7		*0.3*	
	Canopy >0.5 cm	2,3,4,5,6	4	48.2	n.a.	6.5	n.a.
				1.0		*0.3*	
	Duff	8,10,11,13,14	6	31.8	n.a.	3.7	n.a.
				11.7		*1.3*	
	Down wood (DW)	8,9,10,11	4	50.6	n.a.	0.0	n.a.
				1.3		*0.0*	
	Litter	8,9,10-12,11	4	48.9	n.a.	0.1	n.a.
				1.4		*0.0*	
Charred fine residue	Excelsior	1	1	39.0	5.5	4.3	n.a.
	Shrub fuel types	2,3,4,5,	7	20.6	5.8	1.7	n.a.
				13.8	*2.6*	*1.4*	
	Canopy fuel types	6,7,	2	13.0	6.9	1.6	n.a.
				6.3	*2.2*	*0.8*	
	Mix fuel bed types	8,9,10,11	6	33.1	0.1	2.3	n.a.
				8.8	*2.2*	*0.3*	
	Litter fuel type	12	1	37.2	9.7	2.6	n.a.
	Duff fuel type	13,14	3	6.9	0.2	0.6	n.a.
				4.4	*0.8*	*0.3*	
	Charred duff	8,9,10	4	16.0	n.a.	1.1	10.9
				11.8		*0.7*	*4.6*
Charcoal	Charred big DW	8,9,10,11	6	65.2	n.a.	3.5	13.8
				4.1		*0.3*	*3.2*
	Charred small DW	8,9,10,11	6	67.9	n.a.	3.4	15.3
				3.4		*0.5*	*10.3*
	Charred canopy	2,3,4,5,6,8,10,	7	63.9	n.a.	4.1	11.1
				8.8		*1.2*	*6.2*

Note. Standard deviations are given in italics where available. n.a.: not analyzed.

derived from excelsior, litter, and mixed bed fuel types (33–39%, Table 4), while those derived from duff and canopy fuels had the lowest concentrations (7–13%, Table 4). Inorganic C concentrations in the charred fine residue samples were also very variable but were always lower than the organic C concentrations (0–10%, Table 4). The charcoal samples derived from woody materials (i.e., DW or woody canopy) were all enriched in organic C in comparison to the unburnt fuels (64–68% vs. 48–51%; Table 4).

The DSC thermograms for the subset of samples analyzed by TG-DSC are shown in Figure 3, separated between fuel, charred fine residue, and charcoal components. Key parameters obtained from the TG-DSC thermograms for each individual sample are given in Table S1. Thermograms were variable within each of the studied components, but generally, charcoals had a higher thermal recalcitrance than their fuel precursors, with their DSC curves shifted to higher temperatures (Figure 3 and Table S1). This indicates a loss of the most thermolabile compounds (Q1) and enrichment of highly recalcitrant compounds (Q3) during the charring process (Santín et al., 2016). This increase of thermal recalcitrance during charring was not as pronounced in the charred fine residue samples (Figure 3), which were depleted in the most thermolabile compounds relative to the unburnt fuels (Q1; 28.9 ± 6.0% vs. 36.0 ± 7.6%; Table S1), but presented similar Q3% (12.5 ± 5.6% vs. 9.0 ± 6.3%; Table S1). Table S1 also shows the R_{50} values calculated following Harvey et al. (2012). According to this classification, the fuel samples fit into the low C sequestration potential class (Class A, $R_{50} < 0.50$) but most of the charred fine residue (8 of 13) and charcoal (12 of 14) samples fit into Class B ($0.50 \leq R_{50} < 0.70$; Table S1), and, therefore, have "intermediate" C sequestration potentials. None of the PyC samples analyzed here fell within Class C ($R_{50} > 0.70$), which has the highest C sequestration potential, comparable to graphite and soot (Harvey et al., 2012).

For the different types of woody charcoal produced (i.e., from small DW, big DW, and canopy), H:C and O:C molar ratios were calculated and plotted in a van Krevelen diagram (Figure 4). These ratios are commonly

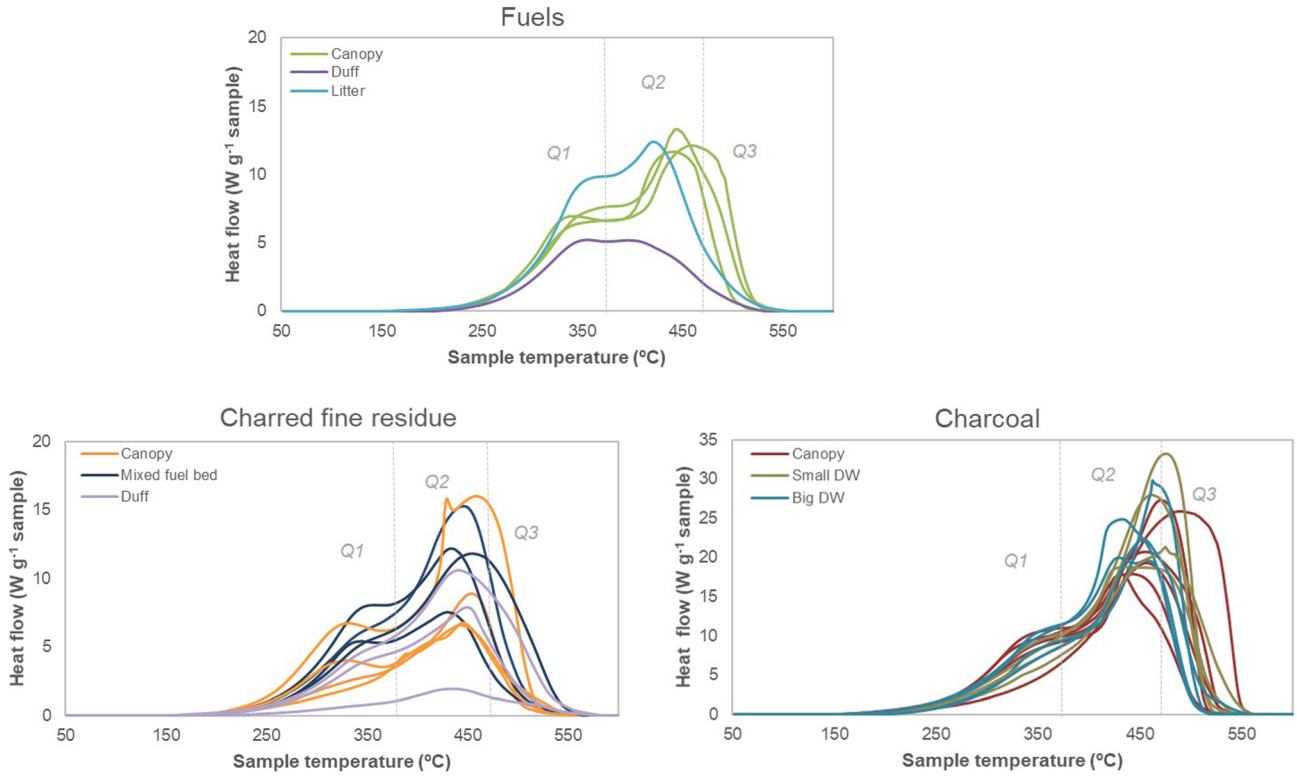

Figure 3. Differential scanning calorimetry thermograms of (top) fuel, (bottom left) "charred fine residue," and (bottom right) charcoal samples. Note different scales for the *y* axes. The dashed vertical lines divide the regions for Q1, Q2, and Q3 (see section 2.3). The line colors identify the main types of the original fuel materials burned. Charred duff samples are included in the "charred fine residue" group as "duff". For the correspondence between each thermogram and its specific sample, see Figure S2. Specific values and key TG-DSC parameters for each sample are given in Table S1.

used as indicators of the degree of carbonization, reflecting condensation (H:C) and oxidation (O:C) (Cao et al., 2013). Figure 4 also shows typical values for feedstocks (i.e., fuels, unburnt vegetation), wildfire charcoals, and biochars from previous studies (Ascough et al., 2011; Kambo & Dutta, 2015; Michelotti & Miesel, 2015; Santín et al., 2017). Compared to wildfire charcoals, FIREX charcoals had similar condensation degrees (i.e., H:C ratios), but much lower oxidation degrees (i.e., O:C ratios, Figure 4), which instead resemble those of biochar materials (Figure 4). These low oxidation degrees indicate that the majority of the products of these fires would be expected to be preserved in environmental matrixes, such as soils or sediments, over long time scales, with half-lives in excess of 1,000 yr (Spokas, 2010), and hence are closer in their characteristics to biochar than to wildfire charcoals (Figure 4). This higher similarity to biochars than to wildfire charcoals may also point to the limitation of the current experiment when attempting to resemble real wildfire conditions (see section 4.1).

3.5. Carbon Emissions Estimations

Carbon emissions accounted for 57–98% of the C contained in the prefire fuels (Table 3). In absolute terms, C emissions varied widely (172–2,127 g C m^{-2}) as a result of very different initial fuel loads (178–2,210 g C m^{-2}; Table S2). In relative terms, the burn of fuel beds with only fine components (Fuels #1 and 12–14, Figure 2) resulted in higher C emissions (90–98% of prefire C) and combustion completeness (96–100%) (Table 3), irrespective of the fire being flaming or smoldering (Table 2). Chaparral fuels (#4 and 5, Table 2) also burnt very completely, resulting in most of the prefire C being emitted (91–95%, Table 3). Excluding the chaparral fuels, the rest of fuel beds with woody components (fuels #2, 3, and 6–11, Figure 2) produced the lowest relative C emissions (57–77% prefire C) and combustion completeness (58–79%, Table 3), mostly due to lower combustion efficiency of the woody fuels (data not shown). Calculation of C emissions using the conventional "consumed biomass" approach instead of the "burnt biomass" approach results in an overestimation of carbon emissions by 2–27% (Table 3).

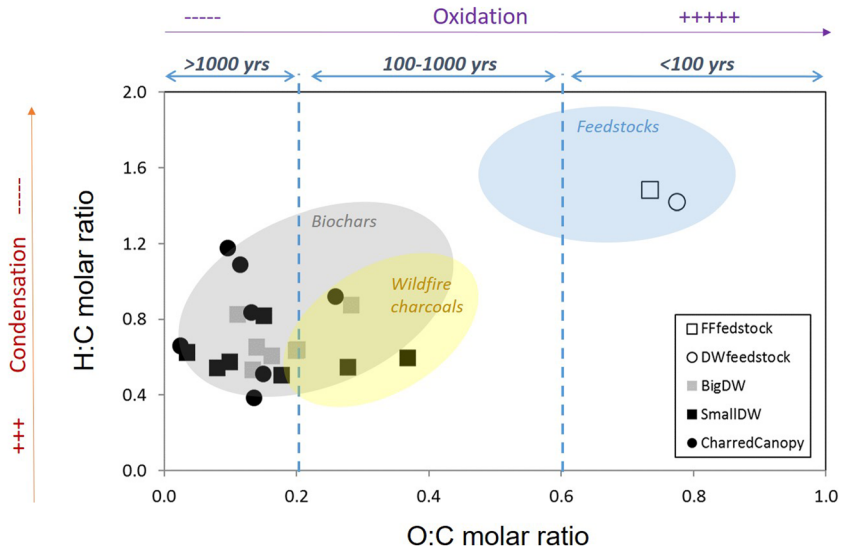

Figure 4. Van Krevelen diagram with H:C and O:C molar ratios for FIREX charcoals and dead wood (DW) and forest floor (FF) feedstocks (from Santín et al., 2017). The areas in blue, gray, and yellow indicate typical values for feedstocks, biochars, and wildfire charcoals, respectively (Ascough et al., 2011; Kambo & Dutta, 2015; Michelotti & Miesel, 2015; Santín et al., 2017). The dotted lines in the *x* axis mark the half-lives ranges (>1,000 yr; 100–1,000 yr; and <100 yr) according to Spokas (2010). Note that "charred canopy" is charcoal derived from small twigs and branches (i.e., no leaf/needle material). "Big DW" is charcoal produced in 100 hr woody fuels (2.5–7.6 cm diameter) and "small DW" is charcoal derived from <100 hr woody fuels (<2.5 cm diameter).

4. Discussion

4.1. PyC Production in Relation to Fire and Fuel Characteristics

Previous studies have found significant relationships between fire behavior parameters and PyC production. For example, Doerr et al. (2018) placed wood pieces on the ground before two boreal forest fires in Canada, one low-intensity (surface fire, <500 kW m^{-1}) and one high-intensity (crowning, ~8,000 kW m^{-1}), and found higher PyC production rates under low-intensity burning, thus, more intense fire producing less PyC in relation to fuel consumed. Similarly, Carvalho et al. (2011), also using woody pieces, found that back fires (lower intensity) formed more PyC than head fires (higher intensity) during prescribed burns in mesic fatwoods in Florida. Wright et al. (2019) also reported a decrease in PyC production with increasing levels of fuel consumption when examining slash pile burns in ponderosa pine-dominated sites in New Mexico and Washington. In a combustion wind tunnel experiment, Surawski et al. (2015) found that flanking and backing fires produced more PyC than heading fires, although the PyC produced during heading fires was more chemically recalcitrant (Surawski et al., 2020). In the present study, PyC production varied widely and we found no correlation between PyC production and combustion completeness (Figure S1), or between maximum temperature and PyC production (Figure S1). In addition, flaming fires did not necessarily produce more (or less) proportion of PyC than smoldering fires (Figure 5).

This lack of conclusive relationships may be related to the very wide range of fuel types used in the present study and to the fact that most burns led to very complete combustion of fuels and, therefore, interburn variability in that respect was rather limited. However, there are some qualitative trends worth highlighting. Overall, fuel beds comprised mostly fine and aerial fuels (shrubs, canopy and litter) and burning under flaming conditions resulted in most C of the fuel burnt by fire being emitted, with only a minor PyC component remaining afterward (Figure 5). Fine fuels that burnt under smoldering conditions (i.e., duff) also had most of the C emitted by fire (Figure 5 and Table 3). The conifer mixed fuel beds presented the highest production of PyC in relation to C emitted (Figure 5). This may relate to the higher proportion of woody fuels in them (Figure 2), as woody fuels generally produce more PyC than fine fuels, especially DW (Jones et al., 2019; Miesel et al., 2018; Santín et al., 2015). Among all fuel types studied, the mixed fuel beds provide the most realistic representation of wildland fuels for common fire-prone conifer forests in North America. The fact

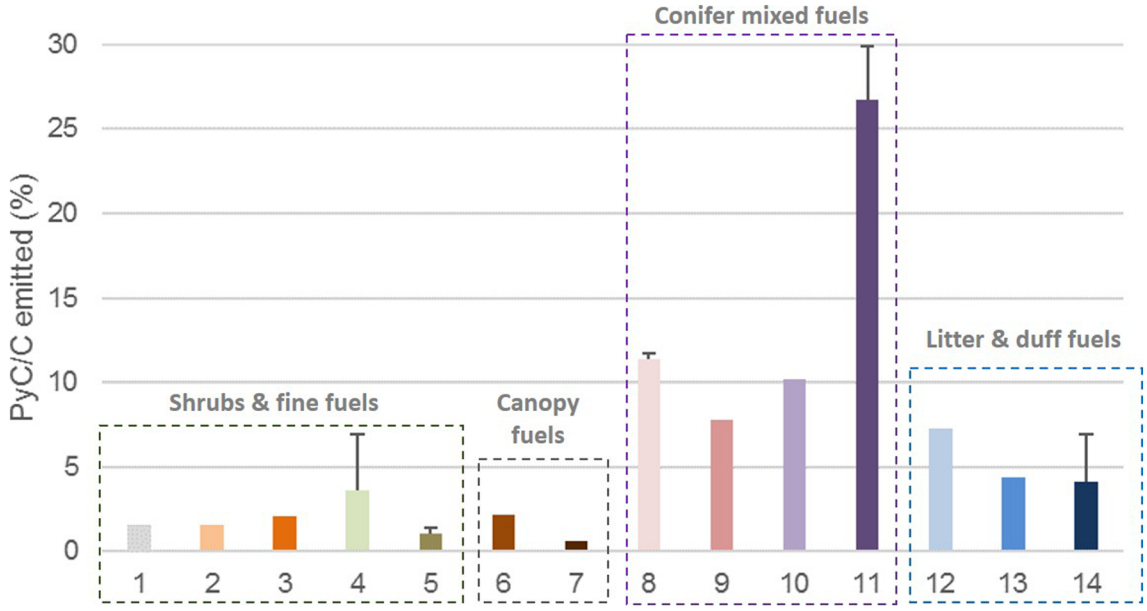

Figure 5. Proportion (%) of pyrogenic C produced in relation to C emitted for the 14 types of fuel beds studied (see Table 1 for fuel bed descriptions). Error bars show standard deviation for fuel beds burnt in more than one fire (see "'Fire number" in Table 3). Different color bars only note different types of fuel beds. For detailed data see Table S2.

that they showed the highest PyC production suggests that PyC production under real wildfire conditions might be quantitatively very relevant in these ecosystems. Miesel et al. (2018) quantified PyC production during wildfires in mixed-conifer forests in California and found around 340 g m^{-2} produced in the tree bark and DW components. Santín et al. (2015) found 480 g m^{-2} formed during a wildfire in a Canadian boreal forest of jack pine in the canopy, DW, and forest floor components combined. DeLuca et al. (2020) recorded a PyC production of 224 g m^{-2} in the forest floor component during a prescribed fire in a thinned ponderosa pine forest in Montana. These rates of PyC productions during wildfire are of the order of 2–19 times greater than the values observed in the experimental mixed fuel beds investigated here (25–166 g m^{-2}, Table S2). This is in part due to a higher proportion of the CB converted to PyC during wildfire, but also to higher pre-fire fuel loads (e.g., 4,280 ± 730 g C m^{-2} in Santín et al., 2015 compared to 178–2,210 g C m^{-2} in the current study, Table S2).

All laboratory burns studied here, with the exception of longleaf pine burns (#96 and 97), generated a relatively low proportion of PyC, with only 1–11% of the fuel C burnt (CB) by fire remaining as PyC (Table 3). These values are lower than those found under field conditions (11–28% CB; Righi et al., 2009; Saiz et al., 2015; Santín et al., 2015) but are within the range of other experimental burns made in the laboratory (0–9% CB; Brewer et al., 2013; Kuhlbusch & Crutzen, 1995). The lower production of PyC under laboratory conditions in comparison to field conditions may result from the higher combustion efficiency generally observed during laboratory burns (Selimovic et al., 2018; Yokelson et al., 2013), as increased combustion efficiency decreases the amount of C left as PyC residues (Carvalho et al., 2011; Doerr et al., 2018). This higher combustion efficiency can be explained by the relatively low moisture content of fuels used (Table S3), underrepresentation of the largest diameter woody fuels, and the small scale of the burns, which increases oxygen availability from the air mass surrounding the fire compared to the conditions present under the much larger burning fuel beds in wildfires. In addition, the fact that the experimental design did not allow replication of the free-moving nature of real fires may have led to different thermokinetics (Sullivan & Ball, 2012). The burning of longleaf pine mixed fuel beds (Fuel 11; #96, 97) were the exception. They resulted in ~21% PyC/CB despite them being characterized by very intense flaming (Figure 1 and Table 3), and fuel moisture, room temperature, and relative humidity being in the range of those in the other burns (Table S3). This indicates that there are clearly other key parameters driving PyC production not accounted for here, such as intrinsic physico-chemical fuel properties (e.g., lignin content or quantity of inorganic

constituents such as silica) or fuel surface/volume ratio, particle size, or fuel bed arrangement (Cornwell et al., 2009; Hudspith et al., 2018).

4.2. Characteristics of PyC Produced

The majority of PyC generated in most of the burns was contained in the charred fine residue component (Figure 2b). This is especially relevant in the wildfire context, where the charred fine residue, commonly named as wildland fire ash, is usually overlooked when investigating C budgets and fluxes from fires. Due to its high mobility in the postfire landscape, both by wind and water erosion, wildland fire ash is often removed from a burnt study site by the time researchers arrive to study fire impacts on C stocks (Bodí et al., 2014; Santín et al., 2012). It is also worth noting that, in some cases, the charred fine residue component had also a substantial amount of inorganic C (although this was always lower than the organic C fraction, Table 3). Inorganic C is a neglected component in research assessing the effects of fire on biogeochemical cycles, probably due both to its high mobility and to widely held assumptions regarding its minor role. Indeed, the inorganic C component in wildland fire ash can actually increase after fire, due to adsorption of atmospheric CO_2 into ash oxides (Balfour et al., 2014).

In quantitative terms, PyC in woody charcoal was not as important as PyC in charred fine residues (Figure 2b), but its chemical and thermal properties suggest that this PyC will have a longer residence time in the environment, and therefore a higher C sequestration potential, than the C contained in the charred fine residue (see section 3.4). This agrees with a previous study that found that the chemical characteristics of the finer PyC particles (<1 mm) makes them more susceptible to microbial degradation (Jenkins et al., 2014). Our assessment of C sequestration potential is only based on chemical and thermal parameters, and we note here that the physical properties of PyC are also important when considering potential residence times in the environment. Physical properties affect the susceptibility of the PyC particles to mobilization and transport to colluvial, fluvial, coastal, and oceanic stores where differing (typically slower) rates of decomposition are observed (Abney & Berhe, 2018; Crawford & Belcher, 2014). Due to the small size distribution of charred fine residue particles, it is thought that finer PyC contained in it may be more susceptible to mobilization at the time scale of days to months than PyC contained on larger charcoal pieces (Scott, 2010).

It is important to bear in mind that the specific fraction of fire-derived organic matter identified and quantified as PyC depends on the isolation technique used (Hammes et al., 2007; Zimmerman & Mitra, 2017). In this study, we used the visual identification method (all material blackened by the fire; Santín et al., 2015), which allows accounting for the whole range of PyC components remaining in situ after a fire. As shown by the TG-DSC analyses, a substantial proportion of some of the studied PyC materials does not show enhanced thermal recalcitrance (Figure 3, Table S1). Indeed, the notion of PyC being almost inert has been disproven in the last decade or so, and PyC has been reconceptualized as a mix of compounds with a range of decomposition susceptibilities and, therefore, ranging C sequestration potentials (Bird et al., 2015). Despite this, many PyC studies still exclusively isolate highly chemically or thermally recalcitrant PyC and therefore miss an important part of the PyC continuum. As an example, in TG-DSC studies, the region 470 and 600°C has been used previously to quantify PyC in environmental matrixes (Edmondson et al., 2015; Hammes et al., 2007), yet this fraction only accounts for 6–43% of the PyC generated during the FIREX FireLab burns (Table S1).

4.3. Implications for C Budget Assessments for Fires

PyC produced during vegetation fires is currently gaining attention as a quantitatively important C sink at the global scale (Jones et al., 2019; Wei et al., 2018). The rationale behind this is that, even if fires release substantial amounts of C into the atmosphere, over the longer term, the C uptake by regenerating vegetation balances the C emissions (except for deforestation and peatland fires) (IPCC, 2013). In addition, PyC materials show longer mean residence times in the environment than their unburnt precursors. Thus, after a complete fire cycle (i.e., including vegetation regrowth), the PyC remaining represents a new C sink (Santín et al., 2016). The final role of PyC as a net C sink will then be determined by the balance between its production and the reduction of PyC stocks by biotic and abiotic degradation (e.g., microbial decomposition, burning by subsequent fires). Changes in fire frequency and extent can be expected to impact both PyC production and removal fluxes, and so projections of rising fire prevalence in the coming century are an

indication that greater quantities of photosynthetically fixed carbon might be sequestered to global stocks of PyC (Jones et al., 2019). The PyC production in the FIREX burns studied here accounted for 1–21% of the C burnt by fire. These values are substantial, but must be taken as a low-end estimate for PyC production by vegetation fires, because the combustion efficiency in these laboratory burns was relatively high compared to actual wildland fire conditions and likely led to lower PyC production rates as discussed above.

In addition to the role of PyC as a C sink, our study also demonstrates that not accounting for PyC production leads to overestimations of C emissions as suggested previously by Surawski et al. (2016). Here, we calculated C emissions for the FIREX burns using the following: (i) the "burnt carbon" approach, which is biogeochemically correct because it accounts for C burnt by fire and converted into PyC and inorganic C instead of being emitted; and (ii) the "consumed biomass" approach, which is the most commonly used, but provides a less accurate approximation of C emission because it assumes that all C in the biomass burnt by fire is emitted (see section 2 for more details). In the current study, we found that the consumed biomass approach leads to overestimation of C emission by 2–27% (with most values between 2–10%; Table 3). Similar to what is discussed above for PyC production, these figures are expected to be higher under real wildland fire conditions, where the combustion of the burnt C will be, under many circumstances, not as complete as during laboratory burns such as the FIREX burns examined here, and therefore, the proportion of C not emitted will be higher. We appreciate that this is a relatively small error when compared to uncertainties affecting fire emission inventories arising from other issues. For example, Nikonovas et al. (2017) reported emissions for large North American wildfires using a range of top-down and bottom-up approaches to vary by a factor of up to 6 and Pan et al. (2019) showed how aerosol emission factors used in global and regional models differ by a factor of 3.8. Notwithstanding these remaining large uncertainties, we argue that, due to the ability of PyC to act as a C sink, this comparatively small error can have significant cumulative consequences in C budgeting exercises focusing on medium- or long-term effects of fires (Jones et al., 2019).

The fact that no correlations were found between the quantities of C emitted and PyC produced, or between the rates of PyC/CB and C combustion completeness among the diverse fuel types and arrangements examined here (Figure S1) can be partially due to the limitations of our experimental setting but, also, highlights once more that the production of PyC during fire is a very complex process that remains poorly understood (Surawski et al., 2020).

5. Conclusions

Constraining uncertainties in C budgets is fundamental to improve our understanding of, and ability to forecast, the impact of wildland fires on local to global C cycles. Here we show that C emission calculations could be improved by accounting for PyC production and by using the "C burnt" approach. Notwithstanding the fact that many other parameters used in fire emission estimates, such area burnt, fuel loads, or emission factors, also present substantial uncertainties (Nikonovas et al., 2017; Pan et al., 2020; Van Der Werf et al., 2017), this improvement can be achieved at relatively little cost and effort for both laboratory and small-scale field burns. For larger scales, ecosystem- or biome-specific-PyC production factors could be applied, as presented in Jones et al. (2019). In addition to the improvement of C emission estimations, data sets of PyC production rates and PyC thermal and chemical recalcitrance, as the ones presented here, are very valuable in allowing a better understanding and modelling of the role of PyC as a C sink in environmental matrixes, such as soils, waters, and sediments. This information is also fundamental for including PyC in Earth System Models to forecast its C sequestration potential over time scales relevant to anthropogenic climate change and its mitigation.

Data Availability Statement

Supporting data sets are available via the Zenodo repository (https://zenodo.org/record/3957830#.XxmiB55KiUk).

Acknowledgments

Special thanks to Bob Yokelson, University of Montana, for making possible the participation of C. S. and S. D. in FIREX 2016 Firelab, and to Jim Reardon, from Missoula Fire Lab, and the laboratory assistants, Edward O'Donnell and Maegan Dills, for their invaluable support during the laboratory burns. Thanks also to Montse Gómez (RIAIDT, University of Santiago de Compostela) who carried out the TG-DSC analyses. C. S. and S. D. received funding support by the Leverhulme Trust Research Grant (RPG-2014-095). C. S. also received funding from the European Union's Horizon 2020 Research and Innovation Programme under the Marie Skłodowska-Curie Grant Agreement 663830 and S. D. from a Leverhulme Trust Research Fellowship (RF-2016-456\2). This work was also supported by NOAA's Climate Research and Health of the Atmosphere Initiative.

References

Abatzoglou, J. T., Williams, A. P., Boschetti, L., Zubkova, M., & Kolden, C. A. (2018). Global patterns of interannual climate–fire relationships. *Global Change Biology*, *24*(11), 5164–5175. https://doi.org/10.1111/gcb.14405

Abney, R. B., & Berhe, A. A. (2018). Pyrogenic carbon erosion: Implications for stock and persistence of pyrogenic carbon in soil. *Frontiers in Earth Science*, *6*(March), 1–16. https://doi.org/10.3389/feart.2018.00026

Akagi, S. K., Yokelson, R. J., Wiedinmyer, C., Alvarado, M. J., Reid, J. S., Karl, T., et al. (2011). Emission factors for open and domestic biomass burning for use in atmospheric models. *Atmospheric Chemistry and Physics*, *11*(9), 4039–4072. https://doi.org/10.5194/acp-11-4039-2011

Ascough, P. L., Bird, M. I., Francis, S. M., Thornton, B., Midwood, A. J., Scott, A. C., & Apperley, D. (2011). Variability in oxidative degradation of charcoal: Influence of production conditions and environmental exposure. *Geochimica et Cosmochimica Acta*, *75*(9), 2361–2378. https://doi.org/10.1016/j.gca.2011.02.002

Balfour, V. N., Doerr, S. H., & Robichaud, P. R. (2014). The temporal evolution of wildfire ash and implications for post-fire infiltration. *International Journal of Wildland Fire*, *23*(5), 733–745. https://doi.org/10.1071/WF13159

Bird, M. I., & Ascough, P. L. (2012). Isotopes in pyrogenic carbon: A review. *Organic Geochemistry*, *42*, 1529–1539. https://doi.org/10.1016/j.orggeochem.2010.09.005

Bird, M. I., Wynn, J. G., Saiz, G., Wurster, C. M., & McBeath, A. (2015). The pyrogenic carbon cycle. *Annual Review of Earth and Planetary Sciences*, *43*(1), 273–298. https://doi.org/10.1146/annurev-earth-060614-105038

Bodí, M. B., Martin, D. A., Balfour, V. N., Santín, C., Doerr, S. H., Pereira, P., et al. (2014). Wildland fire ash: Production, composition and eco-hydro-geomorphic effects. *Earth-Science Reviews*, *130*, 103–127. https://doi.org/10.1016/j.earscirev.2013.12.007

Bond, T. C., Doherty, S. J., Fahey, D. W., Forster, P. M., Berntsen, T., Deangelo, B. J., et al. (2013). Bounding the role of black carbon in the climate system: A scientific assessment. *Journal of Geophysical Research: Atmospheres*, *118*, 5380–5552. https://doi.org/10.1002/jgrd.50171

Brewer, N. W., Smith, A. M. S., Hatten, J. A., Higuera, P. E., Hudak, A. T., Ottmar, R. D., & Tinkham, W. T. (2013). Fuel moisture influences on fire-altered carbon in masticated fuels: An experimental study. *Journal of Geophysical Research: Biogeosciences*, *118*, 30–40. https://doi.org/10.1029/2012JG002079

Campo, J., & Merino, A. (2016). Variations in soil carbon sequestration and their determinants along a precipitation gradient in seasonally dry tropical forest ecosystems. *Global Change Biology*, *22*(5), 1942–1956. https://doi.org/10.1111/gcb.13244

Cao, X., Ro, K. S., Libra, J. a., Kammann, C. I., Lima, I., Berge, N., et al. (2013). Effects of biomass types and carbonization conditions on the chemical characteristics of hydrochars. *Journal of Agricultural and Food Chemistry*, *61*(39), 9401–9411. https://doi.org/10.1021/jf402345k

Carvalho, E. O., Kobziar, L. N., & Putz, F. E. (2011). Fire ignition patterns affect production of charcoal in southern forests. *International Journal of Wildland Fire*, *20*(3), 474–477. https://doi.org/10.1071/WF10061

Core Team, R. (2019). *R: A language and environment for statistical computing. R foundation for statistical computing*. Retrieved from https://www.r-project.org/

Cornwell, W. K., Cornelissen, J. H. C., Allison, S. D., Bauhus, J., Eggleton, P., Preston, C. M., et al. (2009). Plant traits and wood fates across the globe: Rotted, burned, or consumed? *Global Change Biology*, *15*(10), 2431–2449. https://doi.org/10.1111/j.1365-2486.2009.01916.x

Crawford, A. J., & Belcher, C. M. (2014). Charcoal morphometry for paleoecological analysis: The effects of fuel type and transportation on morphological parameters. *Applications in Plant Sciences*, *2*(8), 1,400,004. https://doi.org/10.3732/apps.1400004

DeLuca, T. H., Gundale, M. J., Brimmer, R. J., & Gao, S. (2020). Pyrogenic carbon generation from fire and forest restoration treatments. *Frontiers in Forest and Global Change*, *3*, 24. https://doi.org/10.3389/ffgc.2020.00024

Ditas, J., Ma, N., Zhang, Y., Assmann, D., Neumaier, M., Riede, H., et al. (2018). Strong impact of wildfires on the abundance and aging of black carbon in the lowermost stratosphere. *Proceedings of the National Academy of Sciences of the United States of America*, *115*(50), E11595–E11603. https://doi.org/10.1073/pnas.1806868115

Doerr, S. H., Santín, C., Merino, A., Belcher, C. M., & Baxter, G. (2018). Fire as a removal mechanism of pyrogenic carbon from the environment: Effects of fire and pyrogenic carbon characteristics. *Frontiers in Earth Science*, *6*(October), 1–13. https://doi.org/10.3389/feart.2018.00127

Edmondson, J. L., Stott, I., Potter, J., Lopez-Capel, E., Manning, D. A. C., Gaston, K. J., & Leake, J. R. (2015). Black carbon contribution to organic carbon stocks in urban soil. *Environmental Science and Technology*, *49*(14), 8339–8346. https://doi.org/10.1021/acs.est.5b00313

Gao, B., Taylor, A. R., Searle, E. B., Kumar, P., Ma, Z., Hume, A. M., & Chen, H. Y. H. (2018). Carbon storage declines in old boreal forests irrespective of succession pathway. *Ecosystems*, *21*(6), 1168–1182. https://doi.org/10.1007/s10021-017-0210-4

Hammes, K., Schmidt, M. W. I., Smernik, R. J., Currie, L. a., Ball, W. P., Nguyen, T. H., et al. (2007). Comparison of quantification methods to measure fire-derived (black-elemental) carbon in soils and sediments using reference materials from soil, water, sediment and the atmosphere. *Global Biogeochemical Cycles*, *21*. https://doi.org/10.1029/2006GB002914

Han, Y. M., Can, J. J., Lee, S. C., Ho, K. F., & An, Z. S. (2010). Different characteristics of char and soot in the atmosphere and their ratio as an indicator for source identification in Xi'an, China. *Atmospheric Chemistry and Physics*, *10*, 595–607. https://doi.org/10.5194/acp-10-595-2010

Hantson, S., Arneth, A., Harrison, S. P., Kelley, D. I., Colin Prentice, I., Rabin, S. S., et al. (2016). The status and challenge of global fire modelling. *Biogeosciences*, *13*(11), 3359–3375. https://doi.org/10.5194/bg-13-3359-2016

Harvey, O. R., Kuo, L. J., Zimmerman, A. R., Louchouarn, P., Amonette, J. E., & Herbert, B. E. (2012). An index-based approach to assessing recalcitrance and soil carbon sequestration potential of engineered black carbons (biochars). *Environmental Science and Technology*, *46*(3), 1415–1421. https://doi.org/10.1021/es2040398

Hudspith, V. A., Hadden, R. M., Bartlett, A. I., & Belcher, C. M. (2018). Does fuel type influence the amount of charcoal produced in wildfires? Implications for the fossil record. *Palaeontology*, *61*(2), 159–171. https://doi.org/10.1111/pala.12341

IPCC (2013). Summary for policymakers. *Climate Change 2013: The physical science basis*, *Contribution of Working Group I to the Fifth Assessment Report of the Intergovernmental Panel on Climate Change* (Vol. 33). Cambridge, UK: Cambridge University Press. https://doi.org/10.1017/CBO9781107415324

Jenkins, M. E., Bell, T. L., Norris, J., & Adams, M. A. (2014). Pyrogenic carbon: The influence of particle size and chemical composition on soil carbon release. *International Journal of Wildland Fire*, *23*(7), 1027–1033. https://doi.org/10.1071/WF13189

Jones, M. W., Santín, C., van der Werf, G. R., & Doerr, S. H. (2019). Global fire emissions buffered by the production of pyrogenic carbon. *Nature Geoscience*, *12*(September), 742–747. https://doi.org/10.1038/s41561-019-0403-x

Kambo, H. S., & Dutta, A. (2015). A comparative review of biochar and hydrochar in terms of production, physico-chemical properties and applications. *Renewable and Sustainable Energy Reviews*, *45*, 359–378. https://doi.org/10.1016/j.rser.2015.01.050

Koch, D., Menon, S., Del Genio, A., Ruedy, R., Alienov, I., & Schmidt, G. A. (2009). Distinguishing aerosol impacts on climate over the past century. *Journal of Climate*, *22*(10), 2659–2677. https://doi.org/10.1175/2008JCLI2573.1

Koss, A. R., Sekimoto, K., Gilman, J. B., Selimovic, V., Coggon, M. M., Zarzana, K. J., et al. (2018). Non-methane organic gas emissions from biomass burning: Identification, quantification, and emission factors from PTR-ToF during the FIREX 2016 laboratory experiment. *Atmospheric Chemistry and Physics*, *18*(5), 3299–3319. https://doi.org/10.5194/acp-18-3299-2018

Kuhlbusch, T. A. J., & Crutzen, P. J. (1995). Toward a global estimate of black carbon in residues of vegetation fires representing a sink of atmospheric CO_2 and a source of O_2. *Global Biogeochemical Cycles*, *4*, 491–501. https://doi.org/10.1029/95GB02742

Landry, J.-S., & Matthews, H. D. (2017). The global pyrogenic carbon cycle and its impact on the level of atmospheric CO2 over past and future centuries. *Global Change Biology*, *23*(8), 3205–3218. https://doi.org/10.1111/gcb.13603

Li, H., Lamb, K. D., Schwarz, J. P., Selimovic, V., Yokelson, R. J., McMeeking, G. R., & May, A. A. (2019). Inter-comparison of black carbon measurement methods for simulated open biomass burning emissions. *Atmospheric Environment*, *206*(October 2018), 156–169. https://doi.org/10.1016/j.atmosenv.2019.03.010

McBeath, A. V., Smernik, R. J., & Krull, E. S. (2013). A demonstration of the high variability of chars produced from wood in bushfires. *Organic Geochemistry*, *55*, 38–44. https://doi.org/10.1016/j.orggeochem.2012.11.006

Merino, A., Chávez-vergara, B., Salgado, J., Fonturbel, M. T., García-oliva, F., & Vega, J. A. (2015). Variability in the composition of charred litter generated by wildfire in different ecosystems. *Catena*, *133*, 52–63. https://doi.org/10.1016/j.catena.2015.04.016

Michelotti, L., & Miesel, J. (2015). Source material and concentration of wildfire-produced pyrogenic carbon influence post-fire soil nutrient dynamics. *Forests*, *6*(12), 1325–1342. https://doi.org/10.3390/f6041325

Miesel, J., Reiner, A., Ewell, C., Maestrini, B., & Dickinson, M. (2018). Quantifying changes in total and pyrogenic carbon stocks across fire severity gradients using active wildfire incidents. *Frontiers in Earth Science*, *6*(May), 1–21. https://doi.org/10.3389/feart.2018.00041

Millar, C. I., & Stephenson, N. L. (2015). Temperate forest health in an era of emerging megadisturbance. *Science*, *349*(6250), 823–826. https://doi.org/10.1126/science.aaa9933

Nikonovas, T., North, P. R. J., & Doerr, S. H. (2017). Particulate emissions from large North American wildfires estimated using a new top-down method. *Atmospheric Chemistry and Physics*, *17*(10), 6423–6438. https://doi.org/10.5194/acp-17-6423-2017

Norum, A., & Miller, M. (1984). Measuring fuel moisture content in Alaska: Standard methods and procedures. In *General Technical Reports PNW-171*. (p. 34). Forest Service, Pacific Northwest Forest and Range Experiment Station: U.S. Department of Agriculture. 34 p.

Ottmar, R. D. (2014). Wildland fire emissions, carbon, and climate: Modeling fuel consumption. *Forest Ecology and Management*, *317*, 41–50. https://doi.org/10.1016/j.foreco.2013.06.010

Pan, X., Ichoku, C., Chin, M., Bian, H., Darmenov, A., Colarco, P., et al. (2019). Six global biomass burning emission datasets: intercomparison and application in one global aerosol model. *Atmospheric Chemistry and Physics*, *20*, 969–994. https://doi.org/10.5194/acp-20-969-2020

Pan, X., Ichoku, C., Chin, M., Bian, H., Darmenov, A., Colarco, P., et al. (2020). Six global biomass burning emission datasets: Intercomparison and application in one global aerosol model. *Atmospheric Chemistry and Physics*, *20*(2), 969–994. https://doi.org/10.5194/acp-20-969-2020

Ramanathan, V., & Carmichael, G. (2008). Global and regional climate changes due to black carbon. *Nature Geoscience*, *1*(4), 221–227. https://doi.org/10.1038/ngeo156

Righi, C. A., de Alencastro Graça, P. M. L., Cerri, C. C., Feigl, B. J., & Fearnside, P. M. (2009). Biomass burning in Brazil's Amazonian "arc of deforestation": Burning efficiency and charcoal formation in a fire after mechanized clearing at Feliz Natal, Mato Grosso. *Forest Ecology and Management*, *258*(11), 2535–2546. https://doi.org/10.1016/j.foreco.2009.09.010

Saiz, G., Wynn, J. G., Wurster, C. M., Goodrick, I., Nelson, P. N., & Bird, M. I. (2015). Pyrogenic carbon from tropical savanna burning: Production and stable isotope composition. *Biogeosciences*, *12*(6), 1849–1863. https://doi.org/10.5194/bg-12-1849-2015

Santín, C., & Doerr, S. H. (2016). Fire effects on soils: The human dimension. *Proceedings of the Royal Society B: Biological Sciences*, *371*(1696), 20150171. https://doi.org/10.1098/rstb.2015.0171

Santin, C., & Doerr, S. H. (2019). Carbon. In P. Pereira, M.-S. Jorge, Ú. Xavier, R. Guillermo, & A. Cerdà (Eds.), *Fire effects on soil properties* (pp. 115–128). Clayton, Australia: CSIRO publishing.

Santín, C., Doerr, S. H., Kane, E. S., Masiello, C. A., Ohlson, M., de la Rosa, J. M., et al. (2016). Towards a global assessment of pyrogenic carbon from vegetation fires. *Global Change Biology*, *22*(1), 76–91. https://doi.org/10.1111/gcb.12985

Santín, C., Doerr, S. H., Merino, A., Bucheli, T. D., Bryant, R., Ascough, P., et al. (2017). Carbon sequestration potential and physico-chemical properties differ between wildfire charcoals and slow-pyrolysis biochars. *Scientific Reports*, *7*(1), 11,233–11,211. https://doi.org/10.1038/s41598-017-10455-2

Santín, C., Doerr, S. H., Preston, C. M., & González-Rodríguez, G. (2015). Pyrogenic organic matter production from wildfires: A missing sink in the global carbon cycle. *Global Change Biology*, *21*(4), 1621–1633. https://doi.org/10.1111/gcb.12800

Santín, C., Doerr, S. H., Shakesby, R. A., Bryant, R., Sheridan, G. J., Lane, P. N. J., et al. (2012). Carbon loads, forms and sequestration potential within ash deposits produced by wildfire: New insights from the 2009 "black Saturday" fires, Australia. *European Journal of Forest Research*, *131*(4), 1245–1253. https://doi.org/10.1007/s10342-012-0595-8

Schneider, M. P. W., Pyle, L. A., Clark, K. L., Hockaday, W. C., Masiello, C. A., & Schmidt, M. W. I. (2013). Toward a "molecular thermometer" to estimate the charring temperature of wildland charcoals derived from different biomass sources. *Environmental Science and Technology*, *47*(20), 11,490–11,495. https://doi.org/10.1021/es401430f

Scott, A. C. (2010). Charcoal recognition, taphonomy and uses in palaeoenvironmental analysis. *Palaeogeography, Palaeoclimatology, Palaeoecology*, *291*(1–2), 11–39. https://doi.org/10.1016/j.palaeo.2009.12.012

Sekimoto, K., Koss, A. R., Gilman, J. B., Selimovic, V., Coggon, M. M., Zarzana, K. J., et al. (2018). High-and low-temperature pyrolysis profiles describe volatile organic compound emissions from western US wildfire fuels. *Atmospheric Chemistry and Physics*, *18*(13), 9263–9281. https://doi.org/10.5194/acp-18-9263-2018

Selimovic, V., Yokelson, R. J., Warneke, C., Roberts, J. M., De Gouw, J., Reardon, J., & Griffith, D. W. T. (2018). Aerosol optical properties and trace gas emissions by PAX and OP-FTIR for laboratory-simulated western US wildfires during FIREX. *Atmospheric Chemistry and Physics*, *18*(4), 2929–2948. https://doi.org/10.5194/acp-18-2929-2018

Spokas, K. A. (2010). Review of the stability of biochar in soils: Predictability of O:C molar ratios. *Carbon Management*, *1*(2), 289–303. https://doi.org/10.4155/cmt.10.32

Sullivan, A. L., & Ball, R. (2012). Thermal decomposition and combustion chemistry of cellulosic biomass. *Atmospheric Environment*, *47*, 133–141. https://doi.org/10.1016/j.atmosenv.2011.11.022

Surawski, N. C., Macdonald, L. M., Baldock, J. A., Sullivan, A. L., Roxburgh, S. H., & Polglase, P. J. (2020). Exploring how fire spread mode shapes the composition of pyrogenic carbon from burning forest litter fuels in a combustion wind tunnel. *Science of the Total Environment*, *698*, 134306. https://doi.org/10.1016/j.scitotenv.2019.134306

Surawski, N. C., Sullivan, A. L., Meyer, C. P., Roxburgh, S. H., & Polglase, P. J. (2015). Greenhouse gas emissions from laboratory-scale fires in wildland fuels depend on fire spread mode and phase of combustion. *Atmospheric Chemistry and Physics*, *15*(9), 5259–5273. https://doi.org/10.5194/acp-15-5259-2015

Surawski, N. C., Sullivan, A. L., Roxburgh, S. H., Meyer, C. P. M., & Polglase, P. J. (2016). Incorrect interpretation of carbon mass balance biases global vegetation fire emission estimates. *Nature Communications*, *7*(1), 11536. https://doi.org/10.1038/ncomms11536

Turco, M., Rosa-Cánovas, J. J., Bedia, J., Jerez, S., Montávez, J. P., Llasat, M. C., & Provenzale, A. (2018). Exacerbated fires in Mediterranean Europe due to anthropogenic warming projected with non-stationary climate-fire models. *Nature Communications*, *9*(1), 3821–3829. https://doi.org/10.1038/s41467-018-06358-z

Van Der Werf, G. R., Randerson, J. T., Giglio, L., Van Leeuwen, T. T., Chen, Y., Rogers, B. M., et al. (2017). Global fire emissions estimates during 1997–2016. *Earth System Science Data*, *9*(2), 697–720. https://doi.org/10.5194/essd-9-697-2017

Wei, T. & Simko, V. (2017). *R package "corrplot": Visualization of a correlation matrix* (Version 0.84). Retrieved from https://github.com/taiyun/corrplot

Wei, X., Hayes, D. J., Fraver, S., & Chen, G. (2018). Global pyrogenic carbon production during recent decades has created the potential for a large, long-term sink of atmospheric CO2. *Journal of Geophysical Research: Biogeosciences*, *123*, 3682–3696. https://doi.org/10.1029/2018JG004490

Wright, C. S., Evans, A. M., Grove, S., & Haubensak, K. A. (2019). Pile age and burn season influence fuelbed properties, combustion dynamics, fuel consumption, and charcoal formation when burning hand piles. *Forest Ecology and Management*, *439*(September 2018), 146–158. https://doi.org/10.1016/j.foreco.2019.02.005

Yang, J., Tian, H., Tao, B., Ren, W., Lu, C., Pan, S., et al. (2015). Century-scale patterns and trends of global pyrogenic carbon emissions and fire influences on terrestrial carbon balance. *Global Biogeochemical Cycles*, *29*, 1549–1566. https://doi.org/10.1002/2015GB005160. Received

Yang, Y. Z., Cai, W. H., Yang, J., White, M., & Lhotka, J. M. (2018). Dynamics of postfire aboveground carbon in a chronosequence of chinese boreal larch forests. *Journal of Geophysical Research: Biogeosciences*, *123*, 3490–3506. https://doi.org/10.1029/2018JG004702

Yokelson, R. J., Burling, I. R., Gilman, J. B., Warneke, C., Stockwell, C. E., Gouw, J. D., et al. (2013). Coupling field and laboratory measurements to estimate the emission factors of identified and unidentified trace gases for prescribed fires. *Atmospheric Chemistry and Physics*, *13*(1), 89–116. https://doi.org/10.5194/acp-13-89-2013

Zimmerman, A. R., & Mitra, S. (2017). Trial by fire: On the terminology and methods used in pyrogenic organic carbon research. *Frontiers in Earth Science*, *5*(November). https://doi.org/10.3389/feart.2017.00095